Fractal structures from an evaporation/condensation model

Paul Meakin
Central Research and Development Department,[a] E. I. du Pont de Nemours and Company, Experimental Station, Wilmington, Delaware 19898

J. M. Deutch
Department of Chemistry, Massachusetts Institute of Technology, Cambridge, Massachusetts 02139

(Received 6 May 1985; accepted 8 July 1985)

Several simple evaporation/condensation models in which all occupied surface sites have the same evaporation probability and condensation occurs on contact with the first occupied site have been investigated using Monte Carlo simulations. In two dimensional simulations these models generate a "cloud" of clusters which at long times are characterized by a fractal-like geometry and an exponential cluster size distribution. The nature of the systems at long times depends on the type of trajectories which the particles follow. Brownian trajectories lead to a cloud of clusters with a fractal dimensionality close to 1.0 (in 2D simulations), whereas linear trajectories generate structures with a fractal dimensionality close to 4/3. In similar one dimensional simulations, there is no evidence for the formation of fractal-like structures at any stage in the evolution of the systems and the equilibrium state consists of a dense region and a completely unoccupied region. The results of three dimensional simulations are inconclusive.

INTRODUCTION

A considerable level of interest in growth and aggregation models has recently been stimulated by the Witten–Sander model for diffusion limited aggregation.[1] In the Witten–Sander model, particles follow Brownian (random walk) trajectories originating a large distance from the growing cluster or aggregate. Particles are launched from outside of the region containing the cluster, one at a time and stick on contact with a "seed" site or some part of the growing aggregate. The Witten–Sander model generates fractal-like structures with interesting scaling and universality properties.[1,2] These results have stimulated the development of a number of more or less closely related models.[3–9] In all of these models, the growth process is irreversible and the structures generated are determined solely by the kinetic growth mechanisms. In this paper we present results obtained from a related model in which particles are allowed to add to and evaporate from the "aggregate."

Our model is very similar to the Witten–Sander model for diffusion limited aggregation except that the particle trajectories originate from an occupied interface site on the aggregate. We start with an essentially arbitrary initial state and the system is allowed to reorganize. No particles are added to or taken away from the system during its evolution. Similar simulations have also been carried out in which the particles follow linear (ballistic) trajectories.

We were originally motivated to consider the particle removal as well as addition mechanism by an interest in corrosion and other material loss processes such as etching. However, it is clear that the model discussed in this paper does not simulate this type of process. Here we are simulating the evolution of a simple system towards a steady state. The process is defined in terms of a simple "growth" algorithm which also determines the final state of the system.

SIMULATION METHODS

The unconfined model

The simulation is started by generating an initial state which usually consists of a densely filled "circle" of occupied lattice sites on a square (2d) lattice. To execute a step in the simulation, an occupied lattice site is picked at random and one of its four nearest neighbors is also randomly selected. If the nearest neighbor site is not vacant, a new occupied site is picked at random and this procedure is repeated until a randomly selected occupied site and nearest neighbor unoccupied site have been found. The "particle" occupying the chosen lattice site is moved to the unoccupied site, and this move becomes the first move in a random walk. The random walk continues until the particle reaches a lattice site which has one or more occupied nearest neighbors at which point it sticks. This procedure is repeated many times.

If the moving particle reaches a position which is more than three times the distance of the most distant particle, which is not currently mobile, from the origin, it is moved to a random position on a circle which has a radius a few lattice units larger than that of a circle which just encloses the nonmobile particles. At this stage the simulation becomes very similar to the simulation of diffusion limited aggregation using the Witten–Sander model and the same strategies[2] which were used to reduce computer time requirements in the simulation of 2D. Witten–Sander clusters were used in these simulations also. In some of our simulations, a list of coordinates was maintained for those occupied lattice sites with at least one unoccupied nearest neighbor site (occupied interface sites). However, after a while, almost all of the occupied lattice sites are also interface sites and this procedure was abandoned.

[a] Contribution No.: 5268.

 0021-9606/85/204086-07$02.10

Confined model

In the confined model, the particles or occupied lattice sites are restricted to a finite lattice with periodic boundary conditions. Most of our simulations were carried out on a 512×512 lattice. The simulation is started by randomly occupying N sites on the lattice, avoiding multiple occupancy. The rest of the simulation is very similar to that described above for the unconfined model except that the random walks are confined by the periodic boundary conditions and the average density of the system remains constant.

Linear trajectory model

Simulations similar to those described above can be carried out using linear (ballistic) instead of Brownian (random walk) trajectories. In the case of the unconfined model, the particles leave the region occupied by the initial system permanently and the initial state evaporates. If periodic boundary conditions are used (the confined model), the particles are brought back into the region occupied by the ensemble of particles and the system can reorganize. If the mobile particle did not encounter any other particles before returning to its original position (via the periodic boundary conditions), it was left at its original position.

RESULTS

The unconfined model

Figure 1 shows four stages in a simulation which was started with 5025 particles or occupied lattice sites which approximately form a dense filled circle of radius 40 lattice units. Figure 1(a) shows the system after 50 000 steps. At this stage, the surface has become quite rough, but we still have a compact, almost circular, configuration of particles. In this paper, we use the term "trial" to denote the whole sequence of events which transfers a particle from one position to another. This process includes evaporation, travel along a random walk or linear trajectory, and condensation. Figure 1(b) shows the same simulation after 3 200 000 trials. The central region is still quite dense, but a number of outlying, isolated

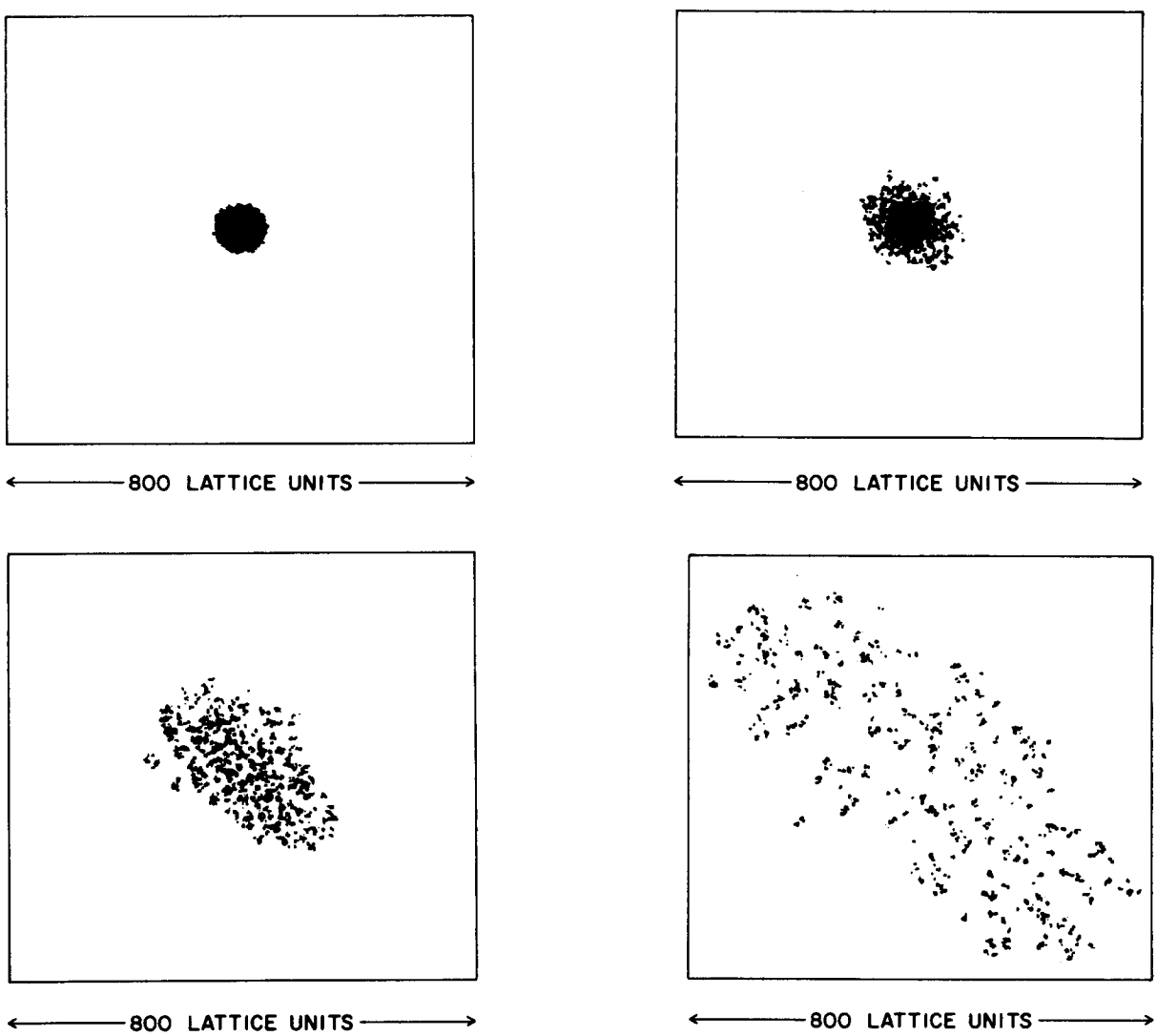

FIG. 1. This figure shows several stages in a two dimensional simulation carried out using the confined model. The initial state for this simulation was a dense circular array of 5025 occupied lattice sites. Figures (a), (b), (c), and (d) show the system after 5×10^4, 3.2×10^6, 1.1×10^7, and 3.8×10^7 trials. Each trial in the simulation consists of a successful, evaporation, random walk, condensation sequence.

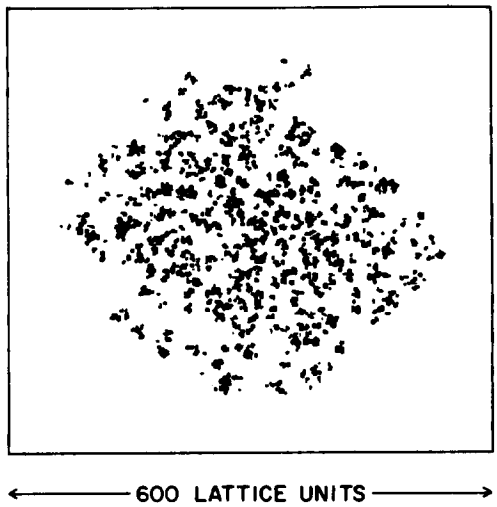

FIG. 2. This figure shows the final state of a simulation similar to that shown in Fig. 1. The initial state consisted of a dense circular array of 7845 particles or occupied lattice sites. The state of the system after 2.24×10^7 steps is shown in this figure.

clusters have developed. After 11 400 000 trials [Fig. 1(c)], the dense central region has disappeared and the overall shape has become quite noncircular. At the end of the simulation [Fig. 1(d)] after 38 000 000 trials (successful random walks), the system has expanded into an oval shape with an overall size of about 400×1000 lattice units. The distribution of occupied lattice sites is extremely nonuniform. Distortion of the initial circular shape seems to be characteristic of this model.

Figure 2 shows the results of a simulation which started with 7845 particles in the form of a densely filled circle of 50 lattice units radius. After 22 400 000 trials the cluster shown in Fig. 2 had evolved. It appears that some distortion from a circular shape is initiated randomly and then amplified by the growth process.

Density–density correlation functions obtained during the simulations used to generate the results shown in Fig. 1 are given in Fig. 3. After a large number of trials, a substantial linear region has developed in the dependence of $\ln C(r)$ on $\ln(r)$ suggesting a fractal-like structure.

The effective fractal dimensionality (D_α)[10] is given by

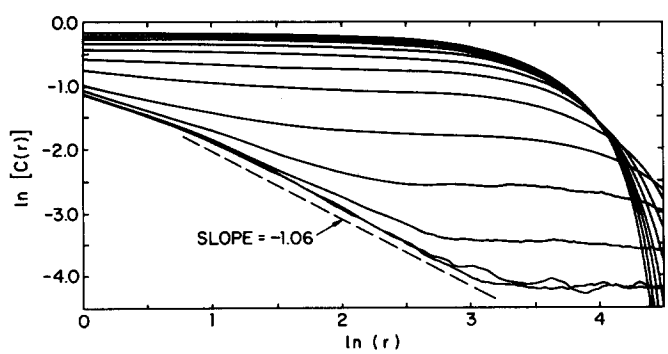

FIG. 3. Density–density correlation functions obtained during the course of the simulation shown in Fig. 1. The correlation functions shown in this figure were obtained after $50\,000 \times 2^m$ trials with $m = 0$, 1–11. The total number of trials in the simulation was $50\,000 \times 2^{11}$ or 1.02×10^8.

$$D_\alpha = d + d\{\ln[C(r)]\}/d[\ln(r)], \quad (1)$$

where d is the Euclidean dimensionality of the lattice. The slope of -1.06 shown in Fig. 3 corresponds to a fractal dimensionality (D_α) of 0.94. Unfortunately, we were not able to extend the results shown in Fig. 3 to a larger number of trials. The results shown in Fig. 3 required about 15 h of CPU time on an IBM 3081 computer. It is quite possible that the efficiency of the computer program could be improved and it would be possible to extend the effective number of trials by reducing the number of particles (at the cost of increased statistical uncertainties). However, instead of pursuing this model further, the confined model was used to obtain more precise quantitative results.

The confined model

Exploratory simulations were carried out with the confined model using 2500, 5000, and 10 000 occupied lattice sites on 512×512 square lattices. Figure 4 presents some of the results obtained using 2500 particles on a 512×512 lattice. From results similar to those shown in Fig. 4 and the corresponding density–density correlation functions, we concluded that the system had closely approached a steady state after about 10^7 trials. Consequently, simulations were carried out in which the density–density correlation function was obtained after each 5×10^5 trials in the range 10^7–2×10^7 trials. The 20 correlation functions were obtained from five such simulations. The log–log plot of the density-density correlation function shown in Fig. 5 is essentially linear over an order of magnitude of length scales. The deviation from linearity at larger distances (r) is attributed to finite concentration effects {at larger r the function $C(r)$ must approach the average particle density ρ of 0.009 537 $[\ln(\rho) = -4.65]$}. Simulations carried out at higher density confirm that the linear region in Fig. 5 will become longer at lower densities. The deviation from linearity at short distances is attributed to lattice and other model details. Such deviations are found in most other growth and aggregation models. The results shown in Fig. 5 indicate that $d\ln[C(r)]/d[\ln(r)] \simeq -1.0$ or $D_\alpha = 2.0 - 1.0 \simeq 1.0$. By least square fitting straight lines to the coordinates $\{\ln[C(r)], \ln(r)\}$ over the range $3 \leqslant r \leqslant 30$ lattice units, the result $D_\alpha = 0.983 \pm 0.049$ was obtained. Similarly, for $4 \leqslant r \leqslant 20$ lattice units we found that $D_\alpha = 0.976 \pm 0.029$. These results were obtained from five simulations carried out using 2500 particles on a 512×512 lattice.

We have also measured the cluster size distribution. Figure 6 shows the results obtained from five simulations carried out with 2500 particles on 515×512 lattices. The cluster size distribution was also obtained by averaging the results obtained after each 10^5 steps in the range 10^7–2×10^7 trials. The results shown in Fig. 6 indicate that the number of clusters of size I (N_1) is related to I by

$$N_I = N_0 e^{-\eta I}, \quad (2)$$

where η has a value of about 1/3. By least squares fitting straight lines to the coordinates $[\ln(N_I), I]$ for each of the five simulations the result $\eta = 0.322 \pm 0.016$ was obtained for clusters in the size range $5 \leqslant N_I \leqslant 20$. Similarly, we found that

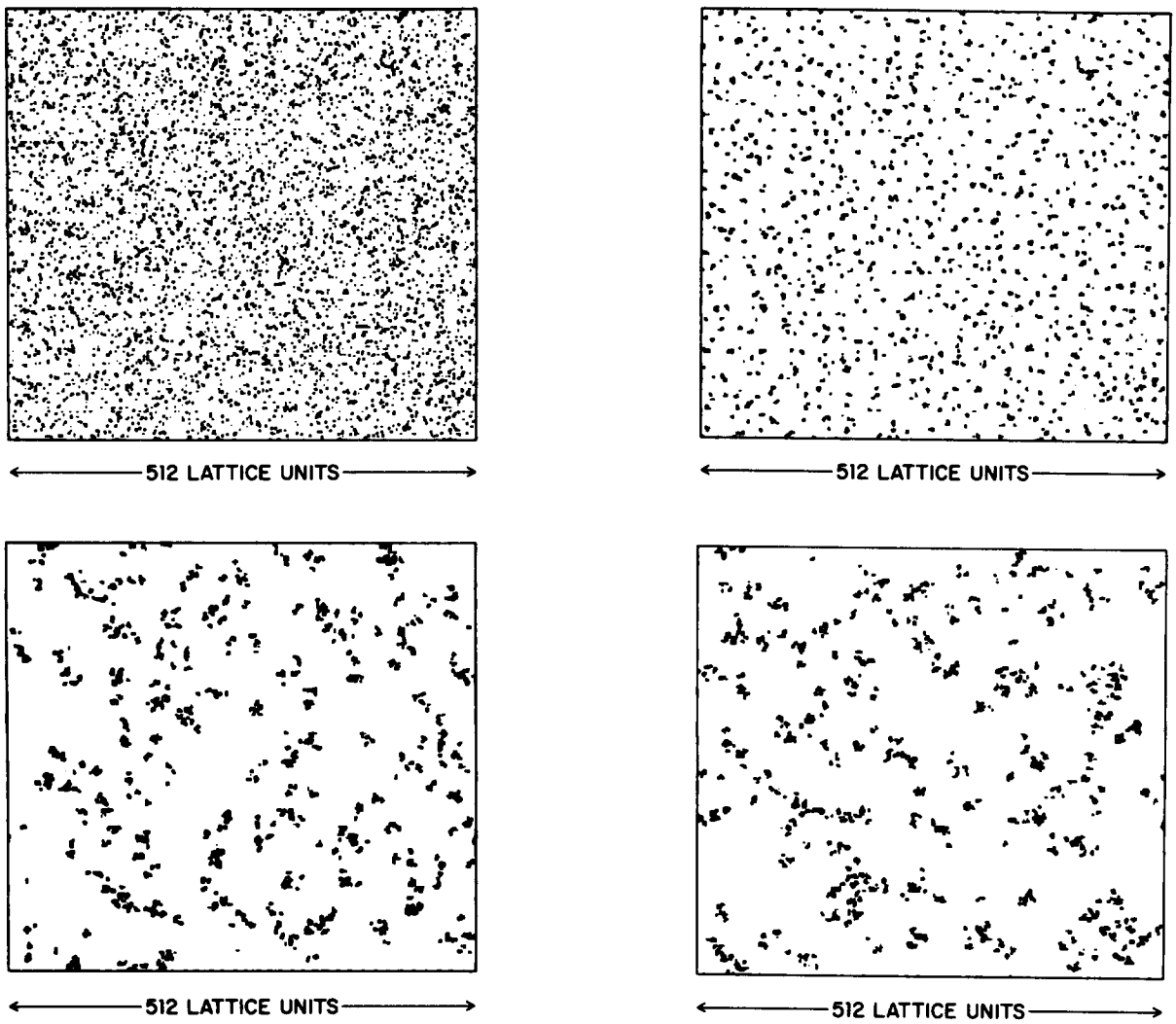

FIG. 4. This figure shows some results obtained using the confined model with 2500 particles on a 512 × 512 lattice. The initial state (a) was obtained by filling 2500 sites on the lattice at random avoiding multiple occupancy. (b), (c), and (d) show what happens after 50 000, 6.4×10^6, and 4.2×10^7 trials, respectively. Random walk particle trajectories were used in this simulation.

$\eta = 0.339 \pm 0.006$ for $3 \leqslant N_I \leqslant 15$ and $\eta = 0.325 \pm 0.022$ for $4 \leqslant N_I \leqslant 25$.

These simulations were carried out using the largest number of trials which were practical. We cannot be absolutely certain that the system does not slowly evolve towards some quite different steady state. However, the fact that similar results were obtained using both the confined and unconfined models with completely different initial states, indicates that a very slow approach to a different steady state is unlikely. In any even, even the transient formation of a fractal-like structure would also be significant and unexpected.

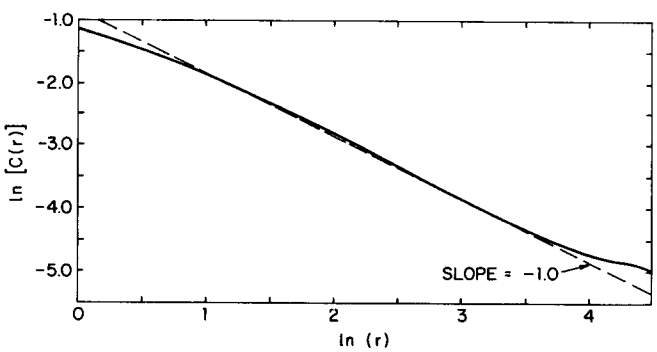

FIG. 5. The density–density correlation function obtained from five simulations carried out using 2500 particles on 512 × 512 lattices with random walk particle trajectories. To obtain the results shown in this figure, correlation functions were determined and averaged for every 5×10^5 steps in the range 10^7–2×10^7 trials.

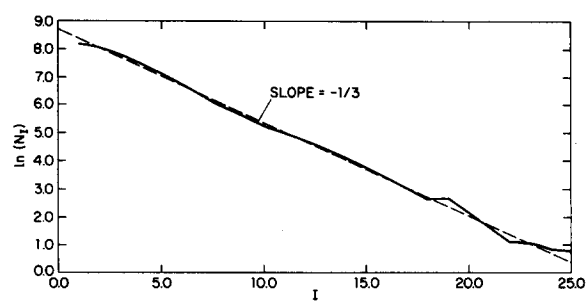

FIG. 6. Cluster size distribution obtained from the simulations used to determine the density–density correlation function shown in Fig. 5. The cluster size distribution functions were averaged in the same way as the density–density correlation functions.

Linear trajectory model

Simulations were carried out using 2500, 5000, and 10 000 particles on 512×512 lattices. All of our results were obtained with a random starting configuration. Figure 7 shows several stages in a simulation carried out using 2500 particles. Most of our simulations were carried out with 5000 particles (a density of 0.0191 particles per lattice site). Figure 8 shows density–density correlation functions obtained after 2.56×10^7, 5.12×10^7, 1.02×10^8, and 1.57×10^8 trials. The results shown in Fig. 8 indicate that the system has reached a steady state with a fractal-like structure after about 2.5×10^7 trials.

In Fig. 9 the density–density correlation functions obtained from simulations at three different particle concentrations are compared. Curve A was obtained from a simulation carried out using 10 000 particles on a 512×512 lattice (0.0381 particles per lattice site). The results obtained after each 2×10^6 trials in the range 5×10^7–10^8 trials were averaged. The noticable deviation from linearity at larger distances in the plots of $\ln[C(r)]$ vs $\ln(r)$ can be attributed to finite concentration effects. Curve B was obtained from a simulation carried out using 5000 particles on a 512×512 lattice. In this case, the density–density correlation functions obtained after each 10^6 trials in the range 4×10^7–8×10^7 were averaged. Curve C was obtained from similar simulations carried out using 2500 particles. In this case, results obtained after each 10^6 trials in the range 2×10^7–4×10^7 trials were averaged. The deviation from linearity at large distances is now attributed to the finite size of the "clouds" of clusters (see Fig. 7). At longer times (when larger clouds of clusters have developed), the linear region extends to longer distances and curve C approaches curve B more closely.

Five simulations were carried out using 5000 particles on 512×512 lattices. The density–density correlation func-

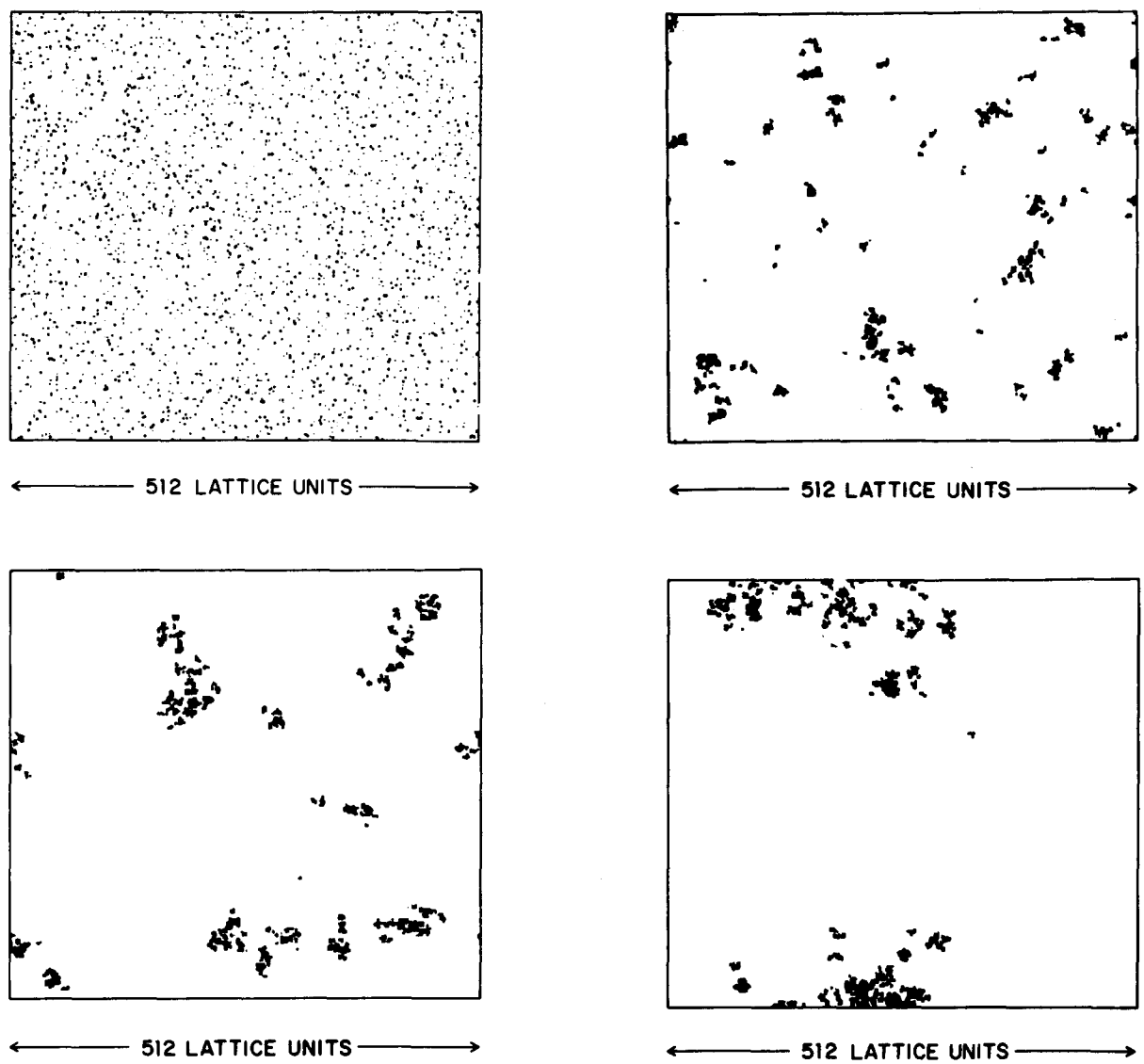

FIG. 7. This figure shows four stages in a two dimensional simulation carried out using the confined model with linear particle trajectories with 2500 particles on a 512×512 square lattice (the six previous figures were obtained using random walk particle trajectories). The results in (a), (b), (c), and (d) were obtained after 0.4×10^5, 3.2×10^6, and 5.12×10^7 trials, respectively.

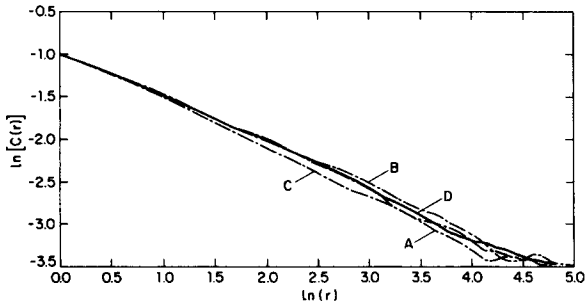

FIG. 8. Density–density correlation functions obtained from a simulation carried out with 5000 particles on a 512 × 512 lattice using linear particle trajectories. Curves A, B, C, and D were obtained after 2.56×10^7, 5.12×10^7, 1.02×10^8, and 1.57×10^8 trials, respectively.

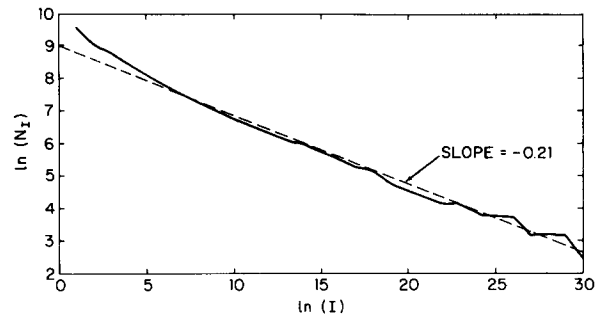

FIG. 10. Cluster size distribution obtained from 2D simulations using linear particle trajectories. The results shown in this figure were obtained from a simulation with 5000 particles on a 512 × 512 lattice. Results obtained after each 10^6 trials in the range 4×10^7–8×10^7 trials were averaged to obtain this figure.

tions obtained after each 10^6 trials in the range 4×10^7–8×10^7 were averaged and straight lines were least squares fitted to the coordinates [ln $C(r)$, ln(r)] over several ranges of length states. In this way, we estimated the effective fractal dimensionality D'_α of the "cluster clouds" to be 1.367 ± 0.048 for $3 < r < 30$ lattice units, 1.383 ± 0.035 for $4 \leqslant r \leqslant 40$ lattice units, and 1.359 ± 0.056 for $2 \leqslant r \leqslant 20$ lattice units.

The cluster size distribution was determined at the same points in the simulations at which the density–density correlation functions were obtained. Figure 10 shows the results from one of these simulations. The results shown in Fig. 10 indicate that the cluster size distribution is exponential.

$$N_I = N_0 e^{-\eta' I}. \tag{3}$$

The constant η' has a value close to 0.21. Other simulations at the same density gave similar results with η' in the range $0.20 < \eta' < 0.25$. Similar results were also obtained at densities of 0.0381 and 0.009 54 particles per lattice site.

ONE DIMENSIONAL MODEL

On a one dimensional, linear lattice, the evaporation/condensation process provides a mechanism for the diffusion of "holes" (unoccupied regions). For both linear and random walk trajectories, holes can coalesce irreversibly.The final state of the system will contain a single dense block of occupied sites which can diffuse very slowly as a result of the evaporation/condensation process. Initially our hope was that simulation in one dimension would help us in understanding the more complicated 2D problem.

Figure 11 shows the density–density correlation functions obtained from a one dimensional simulation carried out using 20 000 particles on a 524 288 (2^{19}) site linear lattice using linear trajectories. Although the maximum number of trials in this simulation is only 160 000, the development of compact regions can already be seen. As the simulation proceeds the region in which $C(r) \simeq 1.0$ (at short distances) will extend to larger distances. There is no reason to believe that a power law relationship between $C(r)$ and r will develop over a significant range of length scales at any stage in the simulations. Figure 12 shows similar results obtained using 20 000 particles on a 2^{20} lattice site linear lattice with Brownian trajectories. Again, our results indicate that the system will evolve into a single region of filled lattice sites with the rest of the lattice totally unoccupied. There is no evidence that the structure of the system will become fractal like at any stage.

THREE DIMENSIONAL SIMULATIONS

Three dimensional simulations have also been carried out. Figure 13 shows the density–density correlation functions obtained from a simulation carried out with 5000 particles on a 100^3 lattice using the confined model with periodic

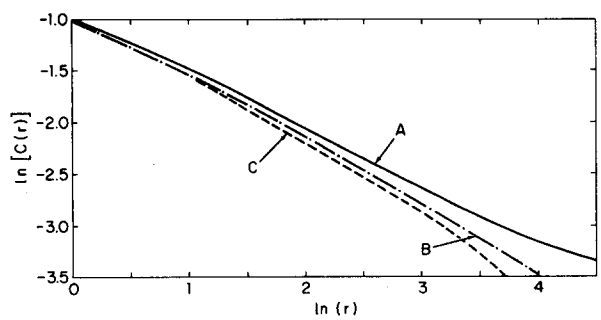

FIG. 9. Density–density correlation functions obtained using linear trajectories on a 512 × 512 lattice at several particle densities. Curve A was obtained using 10 000 particles on a 512 × 512 lattice (particles per lattice site). Curve B was obtained using 5000 particles and curve C was obtained using 2500 particles. Additional details are given in the text.

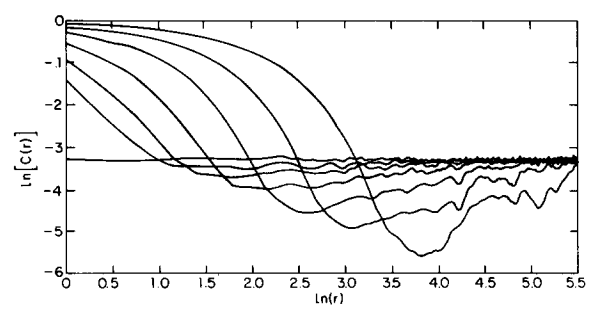

FIG. 11. This figure shows the density–density correlation functions obtained from a one dimensional simulation using 20 000 particles on a 2^{19} site lattice with periodic boundary conditions. Linear trajectories were used in the simulation. The correlation functions are shown after 0, 5000, 10 000, 20 000, 40 000, 80 000, and 160 000 trials.

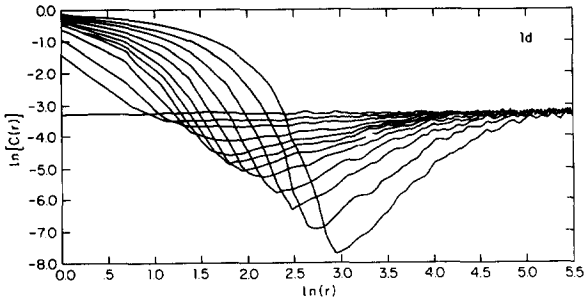

FIG. 12. Density–density correlation functions obtained from a one dimensional simulation carried out with 40 000 particles on a 2^{20} site lattice with periodic boundary conditions. Random walk trajectories were used in this simulation. The correlation functions obtained after 0, 10 000, 20 000, 40 000, 80 000, 160 000, 320 000, 640 000, 1.28×10^6, 2.56×10^6, 5.12×10^6, and 1.02×10^7 trials are shown.

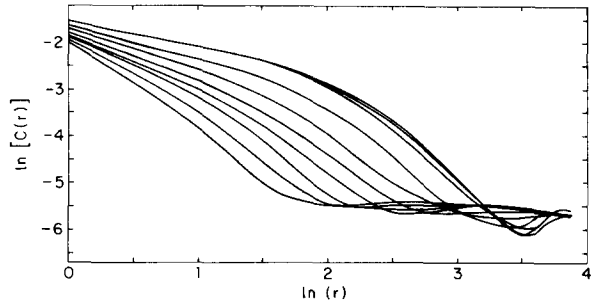

FIG. 13. Density–density correlation functions obtained from the three dimensional confined model with 5000 particles on a 100^3 lattice using random walk particle trajectories. The density–density correlation functions are shown after 5×10^4, 10^5, 2×10^5, 4×10^5, 8×10^5, 1.6×10^6, 3.2×10^6, 6.4×10^6, 1.28×10^7, and 1.36×10^7 trials.

boundary conditions. After more than 10^7 trials, there is no evidence for a substantial linear region in the dependence of $\ln [C(r)]$ on $\ln (r)$. Much longer simulations, (well beyond our present computer resources) would be required to determine if a fractal-like structure eventually develops in the three dimensional system.

SUMMARY AND CONCLUDING REMARKS

This paper presents the results of simulation models which, to our knowledge, for the first time include in particle aggregation models both the possibility of growth and evaporation. The salient result of the two dimensional models for both linear (ballistic) and random (Brownian) particle trajectories is that a steady state appears to be established with a fractal distribution of particles as characterized by the density–density correlation function and an exponential distribution of cluster sizes.

We present these simulation results without explanation for the observations. Accordingly, there are a number of important outstanding unresolved questions which deserve attention. These questions include:

(1) Is the steady state observed in these simulations real or will another final state be approached if a large number of additional trials is undertaken? What is the nature of the steady state which is approached in $d = 3$ and $d > 3$?

(2) Why is a fractal structure formed in this evaporation/condensation model? Can we predict the observed values $D_\alpha \simeq 1.0$ and $\eta \simeq 1/3$ for Brownian trajectories and $D'_a \simeq 4/3$ and $\eta \simeq 0.21$ for linear trajectories in two dimensions?

Finally, we note that an original motivation for studying this problem was an interest in the possibility of the formation of "roughened" or fractal surfaces arising from material loss mechanisms which loosely might be viewed as inversed processes of particle aggregation. We believe this possibility is real and our future efforts will be directed toward constructing and examining the consequences of models which are more faithful to the physics of material loss mechanisms. Recently, models for fluid–fluid displacement in Hele Shaw cells and porous media have been developed in which both evaporation and condensation processes are allowed to occur.[11] It does not appear that our model represents a physically important limit of these fluid–fluid displacement models, but it may be helpful in developing a better fundamental understanding of such processes.

ACKNOWLEDGMENTS

J. M. Deutch acknowledges partial support by the Defense Advanced Research Projects Agency and the National Science Foundation.

[1] T. A. Witten and L. M. Sander, Phys. Rev. Lett. **47**, 1400 (1981).
[2] P. Meakin, Phys. Rev. A **27**, 604, 1495 (1983).
[3] P. A. Rikvold, Phys. Rev. A **26**, 64 (1982).
[4] P. Meakin, Phys. Rev. B **28**, 6718 (1983).
[5] L. Niemeyer, L. Pietronero, and H. J. Wisemann, Phys. Rev. Lett. **52**, 1033 (1984).
[6] P. Meakin, Phys. Rev. Lett. **27**, 2616 (1983).
[7] P. Meakin, Phys. Rev. Lett. **51**, 1119 (1983).
[8] M. Kolb, R. Botet, and R. Jullien, Phys. Rev. Lett. **51**, 1123 (1983).
[9] R. Voss, Phys. Rev. (in press).
[10] B. B. Mandelbrot, *The Fractal Geometry of Nature* (Freeman, San Francisco, 1982).
[11] L. P. Kadanoff (preprint).